XII International Conference on Computational Plasticity. Fundamentals and Applications
COMPLAS XII
E. Oñate, D.R.J. Owen, D. Peric and B. Suárez (Eds)

THE INFLUENCE OF GRAIN SIZE DISTRIBUTION ON STRAIN HARDENING BEHAVIOR FOR DUAL PHASE STEELS USING STATISTICALLY INFORMED ARTIFICIAL MICROSTRUCTURE MODEL AND CRYSTAL PLASTICITY

NAPAT VAJRAGUPTA, JUNHE LIAN, MOHAMED SHARAF, SEBASTIAN MÜNSTERMANN AND WOLFGANG BLECK

Dept. of Ferrous Metallurgy
RWTH Aachen University
Intzestr. 1, 52070 Aachen, Germany
e-mail: napat.vajragupta@iehk.rwth-aachen.de, web page: http://www.iehk.rwth-aachen.de

Key words: Dual phase steels, EBSD, Grain size distribution, Random sequential addition, Multiplicatively weighted Voronoi tessellation.

Abstract. Dual phase steels are well suited to the automotive application. Their microstructures comprise constituents of strong distinction in mechanical properties. As a result, dual phase steels exhibit remarkably high-energy absorption as well as an excellent combination of strength and ductility. Various deformation mechanisms can be observed on the microscale owing to their heterogeneous composition. A reliable microstructure-based simulation approach for describing these deformations is hence needed. Therefore, the approach to generate artificial dual phase microstructure models based on the quantitative results of metallographic microstructure analysis and their statistical representation is developed. This method captures several microstructural features such as microstructure morphology and thus enables a simulation-based analysis of the influence of these features on the meso- and macroscopic material behavior. The algorithm input contains representative information about individual phase grain size and orientation distributions. The statistical parameters to represent the grain size distribution function are then input into a multiplicatively weighted Voronoi tessellation based algorithm to generate artificial microstructure geometry models that are applicable to bimodal distribution and with which microstructure deformation (finite element) simulations can be performed. By implementation of the phenomenological based crystal plasticity model to the generated artificial microstructure model, the influence of grain size distribution on the strain hardening behavior can be investigated.

1. INTRODUCTION

Heterogeneous alloy systems that contain multiple phases possess the potential of reducing structural component weight, energy consumption as well as thermo-mechanical reliability improvement [1]. For this reason, their industrial utilization has significantly increased in the last few decades. However, several sorts of microstructural inhomogeneities exist in these material systems. Among others, preceding forging and differential cooling rates applied result in additional microstructure anisotropy and other irregularities in phase shapes and sizes. As a result, highly heterogeneous finite stress distributions as well as high temperature gradients are present even within large components in application. The component hence usually exhibits local yielding, even at macroscopically elastic loading. Due to the geometrically incompatible regions present in heterogeneous materials and owing to their recent intensive industrial application, robust numerical microstructural modeling has become an essential part of both the material design process and component safety assessment. In other words, the quantitative description of the influence of size and shape of several morphological parameters of the microstructure on the macroscopic performance of components, especially crack initiation and propagation behaviour, is currently an indispensable requirement in science and technology of heterogeneous materials.

There are various application disciplines for the Voronoi tessellation [2], such as astronomy, archaeology, urban planning and physiology, just to mention a few. Recently, Franklin et al. [3] used the Voronoi algorithm in extrapolating 3D microstructure properties from analysis of a 2D micrograph of a rail steel and used the resulting geometry model in determining obstacles to crack propagation. Nygards et al. [4] presented micromechanical FE simulations with a ferrite/pearlite steel and employed the Voronoi algorithm to produce periodic representative volume elements (RVEs). However, although the material analyzed in the latter study is a dual phase steel, the statistical data considered in the Voronoi algorithm only corresponded to the microstructure as a whole. This is to say, the Voronoi algorithm employed generated the geometry model without differentiating between different phases, so that the statistical parameters (e.g. grain size/orientation distribution) of each phase cannot be individually altered. Very recently, Regener et al. [5] presented an approach that solved this issue. They applied the more sophisticated Johnson-Mehl tessellation in order to capture the characteristic phase dimensions, among other purposes. The current study presents a mathematically adaptive algorithm, based on the relatively simpler multiplicative Voronoi tessellation [6], which allows for the simulation of dual grain phase evolution during solidification of metal melt and considers the statistical data of each phase in the microstructure individually.

The next chapter of the paper describes the algorithm in detail, the implementation results and interesting features of the offered algorithm. In chapter 3, plasticity parameters calibration procedure for the constituents is presented. The paper closes with concluding remarks and suggestions of generalization and future work.

2. THE STATISTICALLY INFORMED ARTIFICIAL MICROSTRUCTURE MODEL

2.1. Statistical representation of the microstructure features

To begin with, DP600 steel with an ultimate tensile strength of 600 MPa was investigated by electron backscatter diffraction (EBSD) [7]. In the micrograph as shown in **Figure 4**, the coloured grains are ferrite and the black grains are martensite. From the micrograph, the grain diameters are measured in order to determine the appropriate distribution function with adequate statistical parameters for each of the two mentioned microstructure constituents. Due to the irregularity of grain shape, the maximum and minimum grain diameters are measured and the average is used as grain size data. By fitting the grain size data with a method for fitting a univariate distribution of non-local scale family using a cumulative distribution function [8], log-normal distribution function well describe the grain size distribution of both phases. The log-normal distribution function [9] is introduced to take the asymmetry or the skewness of the measured data into account. The probability density function of log-normal distribution function is described as

$$f(x) = \frac{1}{S\sqrt{2\pi}x} e^{-\frac{(\ln x - M)^2}{2S^2}}, x > 0 \tag{1}$$

where M and S can be calculated from $\mu_{\text{log-}normal}$ and $\sigma_{\text{log-}normal}$ which are mean and standard deviation for the log-normal distribution function, respectively:

$$M = \ln\left(\mu_{\text{log}-normal}^2 / \sqrt{\sigma_{\text{log}-normal}^2 + \mu_{\text{log}-normal}^2}\right), \tag{2}$$

$$S = \sqrt{\ln\left(\left(\sigma_{\text{log}-normal} / \mu_{\text{log}-normal}\right)^2 + 1\right)}. \tag{3}$$

Table. 1 shows the estimated statistical parameters for ferrite and martensite. Furthermore, the obtained parameters are used to plot the distribution function in order to compare the values to the grain size histograms of both phases. These comparisons are illustrated in **Figure 1** and **Figure 2** respectively for the ferritic and the martensitic phase.

	M, µm	S, -	μ, µm	σ, -
Ferrite	1.506	0.599	5.390	3.541
Martensite	0.015	0.839	1.440	1.459

Table 1: Summary of the estimated statistical parameters for ferrite and martensite.

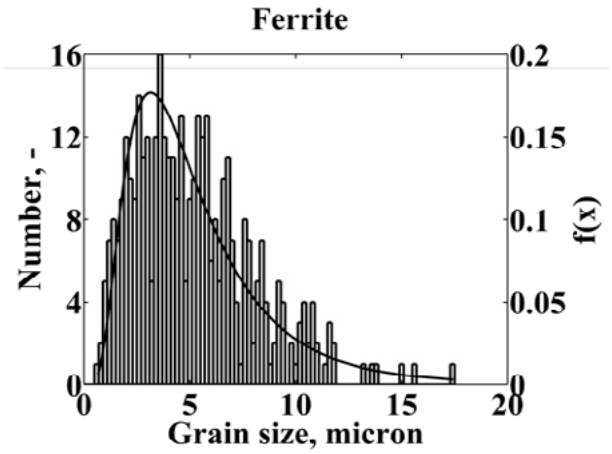

Figure 1: Comparison between the grain size histogram with the log-normal distribution function calculated by estimated statistical parameters for ferrite.

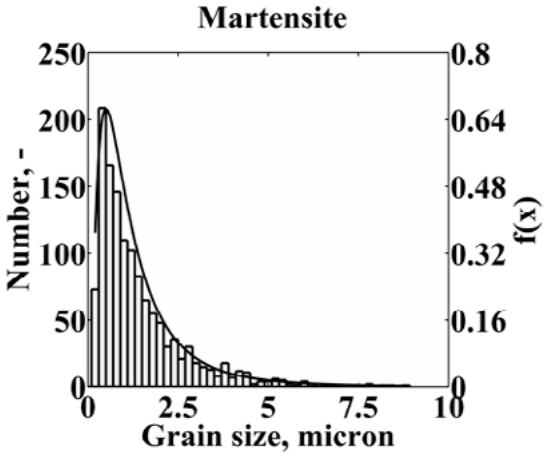

Figure 2: Comparison between the grain size histogram with the log-normal distribution function calculated by estimated statistical parameters for martensite.

After the statistical parameters of adequate distribution functions are obtained, these parameters - together with the defined microstructure size - are used as input parameters for calculating numbers of grains that should be generated at the specific size. First, the number fraction *n(x)* is calculated from the distribution function. Afterwards, the area fraction *a(x)* is converted from *n(x)* and the number of grains that have to be created at specific size *k(x)* can be attained from *a(x)* respectively.

Since the cumulative distribution function, CDF is defined as the area so far under the probability density function, the subtraction of the CDF of x from the CDF of $x+dx$ results in the interval area under the probability density function between x and $x+dx$. In the other words, the interval area can be calculated from the new derivation and the number fraction *n(x)* can be obtained. This derivation for the number fraction reads

$$n(x) = F_{\log-normal}(x+dx) - F_{\log-normal}(x)\,. \tag{4}$$

This yields:

$$n(x) = \frac{1}{2} erfc\left[-\frac{\ln(x+dx)-\mu}{\sigma\sqrt{2}}\right] - \frac{1}{2} erfc\left[-\frac{\ln x-\mu}{\sigma\sqrt{2}}\right]. \tag{5}$$

Then, *n(x)* is converted into an area fraction *a(x)*. *n(x)* is initially multiplied with the area x^2, which is fully occupied by a grain with diameter x. This product is then divided by the summation of the product of the area of grain x_i^2 with diameter x_i and the corresponding number fraction $n(x_i)$,

$$a(x) = \frac{x^2 \cdot n(x)}{\sum_{i=1}^{n} \left[x_i^2 \cdot n(x_i) \right]}. \tag{6}$$

Thus, the number of grains to be generated at specific size *k(x)* can be calculated in the following last step. It starts by multiplying *a(x)* with the defined RVE area A_{RVE} and the phase fraction of the selected phase N_α. This multiplication expresses the total area of grains occupying the RVE space. Then, the term is divided by the area of each grain,

$$k(x) = \frac{a(x)}{x^2} \cdot A_{RVE} \cdot N_\alpha \quad . \tag{7}$$

The result from the calculation is then used in a seeding procedure by applying the random sequential addition algorithm and multiplicatively weighted Voronoi tessellation respectively.

2.2. Multiplicatively weighted Voronoi tessellation

Before the seeds or kernels, which are the main input of the ordinary Voronoi tessellation, are placed in the defined RVE space, they are correlated to the characterized grain size distribution function. This is a crucial step to finally achieve the desired grain size distribution in the RVE. The number of seeds is determined according to the number of grains to be generated. Circles are then defined around the seeds reserving a space where no other seed may be placed. The diameters of these circles are directly proportional to the grain size diameters in order to represent the grain size distribution function as determined earlier. Next, the seeds and their corresponding circles are placed into the defined RVE area by applying the random sequential addition algorithm (RSA) [10-11]. The principle of RSA algorithm follows three major rules:

- Objects are inserted into the defined d-dimensional volume randomly and sequentially.
- Objects may not overlap.
- As soon as the object is inserted, it is clamped in its position and cannot be moved or removed from the defined d-dimensional volume.

Based on the third rule, the RSA algorithm is an irreversible process. Nevertheless, it might happen that some seeds lie in the reserved space of the RVE, but at least a part of its corresponding circle reaches out of this space. Only in such case, the seed would be repositioned. After the process is completed, positions of seeds and diameters are used as input parameters for the construction of the microstructure geometry model by applying the multiplicatively weighted Voronoi tessellation in a further step. **Figure 3** illustrates seeds and corresponding circles fitted into the defined RVE space. As it can be observed, they can be perfectly fitted into the defined RVE space with the RSA algorithm.

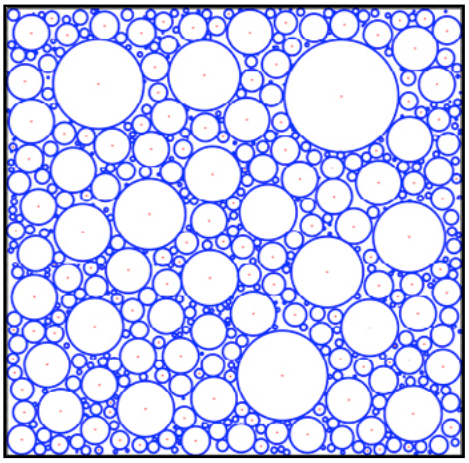

Figure 3: Seed circles fitted into the defined RVE space with RSA algorithm.

With the seed circles being placed into the RVE space, positions and diameters are used as input parameters to the multiplicatively weighted voronoi tessellation (MW-voronoi) [2]. With MW-voronoi, every seed points have got a specific weight reflecting the variable property of the seeds. Therefore, the grain diameter is assigned to the tessellation algorithm as weight property in order to manipulate the generated grain size. However, due to the complexity of the grain shape after the tessellation algorithm is executed which is described as a set of arc, a simplification of the geometry is required. To simplify the geometry for grains construction, the stored arc data is approximated by a linear form. As a result, the generated artificial microstructure model created by the mentioned algorithms is shown in **Figure 4**. Herein, the colours represent different orientations of ferrite grains, while the white grains represent the martensitic phase, since no orientation is assigned for the case of martensite.

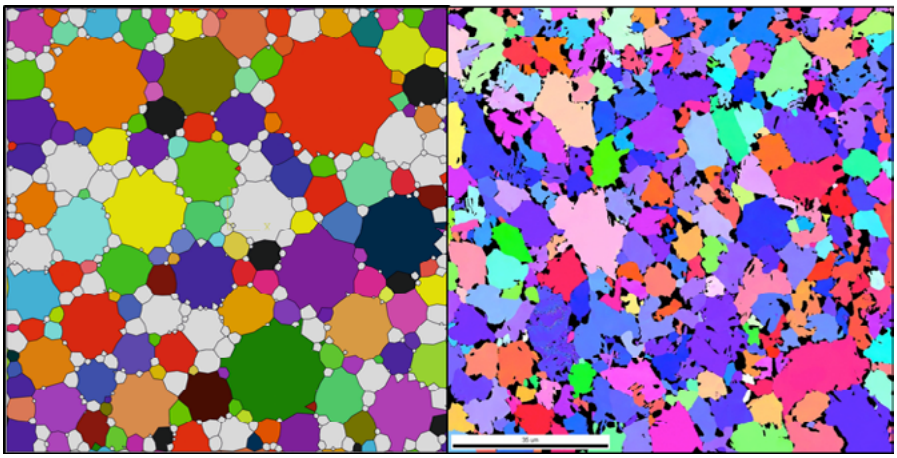

Figure 4: The artificial microstructure model (left) and comparison to the microstructure characterized by EBSD analysis (right).

To assess the precision of the microstructure model generation with the presented approach, the phase fractions of both phases are measured. The comparison between the

EBSD result and the one calculated from the artificial microstructure is shown in **Table 2**. Obviously, the phase fractions from the microstructure model only slightly deviate from the microstructure characterization result.

	Phase fraction, %	
	Ferrite	**Martensite**
Microstructure characterization	78	22
Artificial microstructure model	79	21

Table 2: Phase fraction comparison between result from microstructure characterization and calculated from the artificial microstructure model [12].

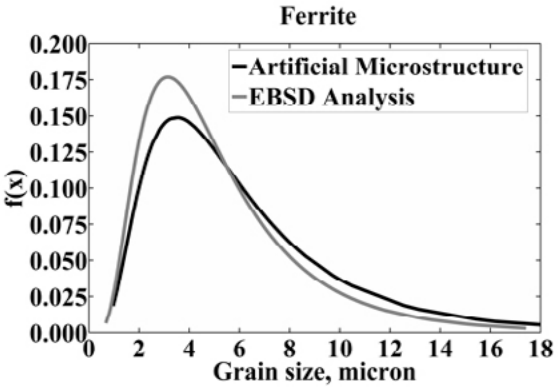

Figure 5: Comparison between the grain size distribution functions of ferrite approximated from EBSD analysis result and from the artificial microstructure.

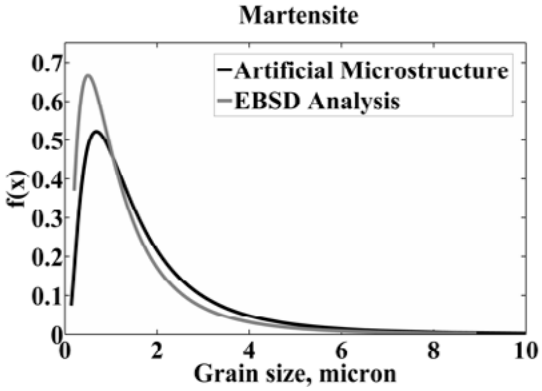

Figure 6: Comparison between the grain size distribution functions of martensite approximated from EBSD analysis result and from the artificial microstructure.

Moreover, the diameters of generated grains are stored for each phase and fitted to the distribution functions according to the approach presented earlier in this paper. **Figure 5** and **Figure 6** show the log-normal grain size distribution functions of ferrite and martensite; both for the real and the artificial microstructures. From these diagrams it can be concluded that the curves representing the artificial microstructure seem to be in a good agreement when compared to the curves representing EBSD analysis.

2.3. Influence of statistical parameters on the generated artificial microstructure model

In addition to the purpose of artificial microstructure generation based on the estimated statistical parameters from quantitative microstructure characterization, the current algorithm can also be used to create "virtual" of "tailored" microstructure models. This becomes interesting for application in the field of integrative computational materials engineering, where microstructure configurations are designed targeting certain mechanical properties on the full-component scale. For the generation of these microstructure models, the normal distribution function is implemented to ferrite and martensite in order to simplify the calculation. Two sets of statistical parameters including different average grain diameters of both phases are implemented to the algorithm. Figure 8 shows the artificial microstructures derived from different sets of statistical parameters. The grey grains refer to martensite and the coloured grains represent the randomly oriented ferritic grains.

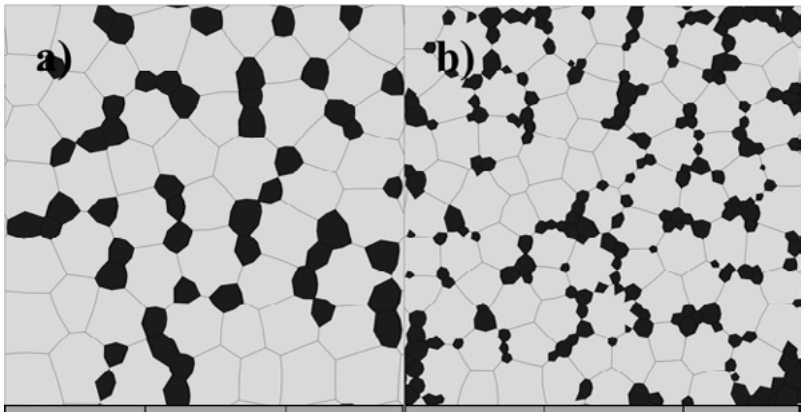

	μ, µm	σ, -		μ, µm	σ, -
Ferrite	5.00	0.40	**Ferrite**	4.00	0.40
Martensite	2.50	0.30	**Martensite**	1.20	0.30

Figure 8: Artificial microstructure with different sets of statistical parameters; a) μ_1=5.00 µm, μ_2=2.50 µm, σ_1=0.40 and σ_1=0.30, b) μ_1=4.00 µm, μ_2=1.20 µm, σ_1=0.40 and σ_1=0.30.

3. PLASTICITY PARAMETERS CALIBRATION FOR THE CONSTITUENTS

To determine the plasticity parameters of the constituents, 2 different derivation schemes are deployed. For ferrite, Nano-indentation test is performed in order to obtained crystal plasticity parameters. In the recent years, crystal plasticity model has been intensively developed and applied to simulate the material behavior of the single crystal or polycrystal taking the crystallographic orientations of grains into account [12-14]. In the past, the crystal plasticity parameters for single crystal were mainly identified by inverse fitting on a polycrystal aggregate incorporating to certain homogenization scheme in matching the flow curve determined from the tensile test with finite simulation result [15-16]. Nevertheless, this procedure cannot be applied to DP steels in which 2 crystal structures are found. With the help of Nano-indentation test, it opens door to directly characterize the material behavior of a single crystal within a polycrystal [14]. In other words, it can capture behavior of each constituent in the microstructure. Therefore, Nano-indentation test with a spherical-conical indenter (tip radius of 1 µm) is conducted on a single ferritic grain of DP steel. The material deformation behavior, such as the load-depth curve and the surface topography of the pile-ups are, respectively, recorded simultaneously measured by scanning probe microscopy (SPM) as post-processing. Simulations of Nano-indentation test in a crystal scale are performed in finite element (FE) code, Abaqus, incorporating to the crystal plasticity model to calibrate the corresponding material parameters.

To calibrate the crystal plasticity parameters for ferrite in the DP steel, the Nano-indentation test with a spherical-conical indenter (tip radius of 1 µm) is conducted. During the test, the load-depth response of the indented was simultaneously recorded and depicted. After the Nano-indentation tests, the sample is scanned in the same system by SPM technique to obtain the surface topographies and pile-up profiles. **Figure 9** shows the SPM images for the indented grain. From the Nano-indentation test results, a 3D finite element (FE) model, as shown in **Figure 10**, is constructed in the commercial FE code Abaqus/Standard [17] for the

simulation of Nano-indentation test. Due to the symmetries, one eighth of the whole setup is considered. The indenter is modeled as a rigid body and the contact interaction between indenter and specimen is assumed frictionless. Due to the high concentration of local variables underneath the indenter, a finer mesh is used near the indenter tip and a coarser mesh is used for other regions. The element type for the model is defined as 8-node linear brick (C3D8). The previously described crystal plasticity model is incorporated into the model as a user defined subroutine (UMAT). From the constructed model, the crystal plasticity parameters are calibrated to fit the shape of the pile-ups and the load-depth plot.

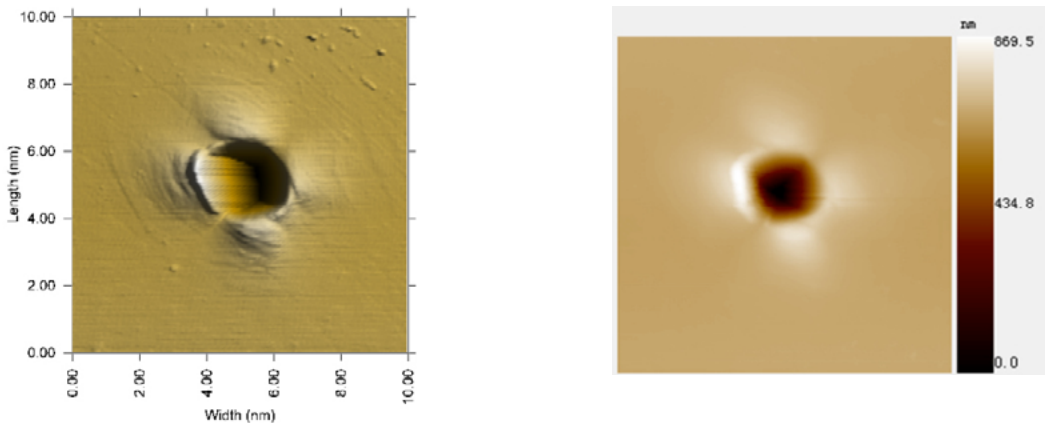

Figure 9: SPM images (left: top view of the indent, right: the same view with the contour of the out-of-plane displacement) of the indent impressions made by a spherical-conical indenter (tip radius 1.0 µm) [18]

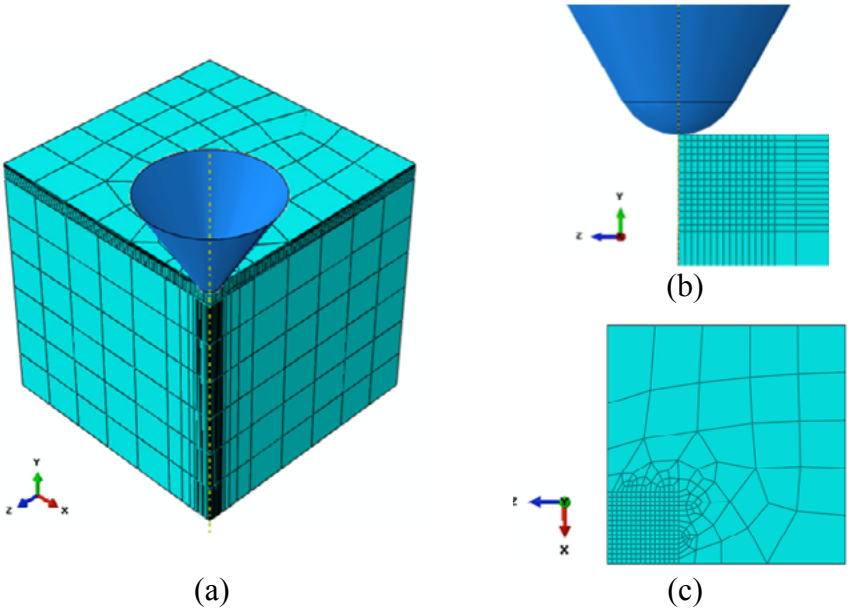

Figure 10: 3D FEM nanoindentation model setup in Abaqus: (a) overall view; (b) latent view at the part beneath the indenter tip; (c) top view of the single crystal without indenter. [18]

After the calibration process, the comparison of load-depth response between experimental results and numerical prediction is plotted in **Figure 11**. Furthermore, The distributions of the

out-of-plane displacements on the surface of the indents obtained from CPFEM simulations for both grains are presented in **Figure 12**. The pattern of the pile-ups coincides with the experimental results. Despite some deviations, an overall good agreement is achieved.

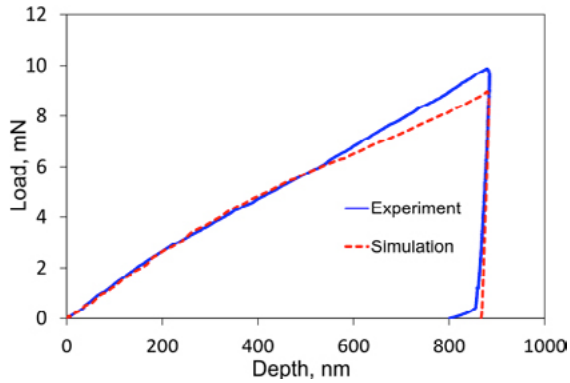

Figure 11: Comparison of the load–depth curve between experimental and numerical results for the indentation test. [18]

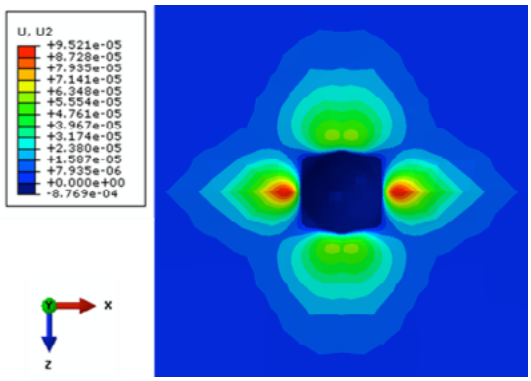

Figure 12: Surface topographies of out-of-plane displacements of CP simulations of nanoindentation tests with the calibrated parameters. [18]

Because the average grain size of martensite is approximately 1 µm, it is not possible to perform the Nano-indentation test into such a small grain. Furthermore, the martensite grains also consist of several sub-structures with different sets of orientation. Therefore, there should be simplified alternative for derive the strain hardening behavior for the martensitic phase. To cope with this requirement, an approximation of empirical model was applied. This empirical model neglects the orientation and is derived based on dislocation theory. With this approach, the Peierl's stress is computed empirically according to the local chemical composition [19-23]. The approach is given as,

$$\sigma = \sigma_0 + \Delta\sigma + \alpha \cdot M \cdot \mu \cdot \sqrt{b} \cdot \sqrt{\frac{1-\exp(-M \cdot k \cdot \varepsilon)}{k \cdot L}}, \tag{8}$$

α is a constant, M is a Taylor factor (M=0.3), μ is the shear modulus (μ=80000 MPa) and b is the Burger's vector $\left(b = 2.5 \cdot 10^{-10} m\right)$. L is the dislocation mean free path, k is the recovery rate and $\Delta\sigma$ is the additional strengthening with regard to precipitations and carbon in solution. σ_0 is the Peierl's stress, which depends on the chemical constituents of the material in a solid solution, and is presented in Eqs. (9), whereas N_{ss} is nitrogen content in solid solution.

$$\begin{aligned}\sigma_0 &= 77 + 80 \cdot (\%Mn) + 750 \cdot (\%P) + 60 \cdot (\%Si) \\ &+ 80 \cdot (\%Cu) + 45 \cdot (\%Ni) + 60 \cdot (\%Cr) + 11 \cdot (\%Mo) + 5000 \cdot N_{ss}\end{aligned} \tag{9}$$

Since modeling of the strain-hardening behavior with this approach is highly influenced by the local concentration of alloying elements, the carbon partitioning was estimated based on a

mass balance and an evaluation of the phase fractions. **Table 3** summarizes all the constants used for each phases. The modeled flow curves of martensite regarding the aforementioned models can be found in **Figure 13**.

%C	s_0	$\Delta\sigma$	α	M	b	μ	k	L
0.41	236.8	1082.65	0.33	3.0	2.5×10^{-10}	80000	41	3.8×10^{-8}

Table 3: Summary of all model constants for flow curves prediction of martensite.

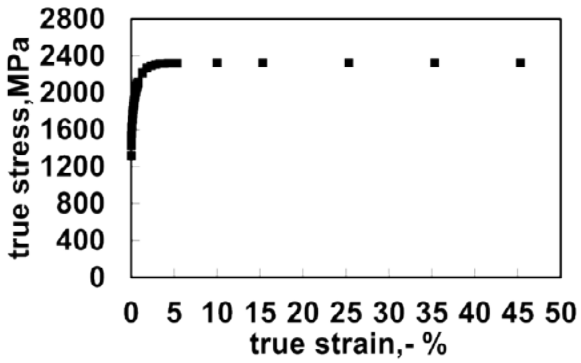

Figure 13: Modelled flow curves for martensite of the investigated dp steel.

4. CONCLUSIONS

- The aim of this study is to study the influence of grain size distribution on the deformation and strain hardening behavior. To achieve this aim, the statistically informed artificial microstructure model is generated.
- This artificial microstructure model is based on the multiplicatively weighted voronoi tessellation with statistical parameters of individual phase grain size and orientation distribution functions as input parameters.
- With statistical input parameters, seeds treated as seed circles with diameters reflecting the measured grain sizes are generated accordingly and placed into the defined RVE space according to RSA algorithm. The position and diameter of the seed circles is later considered during the multiplicatively weighted Voronoi tessellation algorithm.
- The phase fractions and the grain size distribution functions of the artificial microstructure model shows a good agreement to the values derived for the real microstructure in the EBSD analysis.
- The grain sizes for both phases of the generated microstructure can be manipulated by varying the statistical input parameters. With the feature of the algorithm, influence of the grain size distribution on mechanical behaviour can be investigated.

- To determine the plasticity parameters of the constituents, different derivation schemes are deployed. For ferrite, nano-indentation test is performed in order to obtained crystal plasticity parameters. For martensite, an approximation of empirical model based on the local chemical compositions was applied.
- By implementing plasticity parameters of the constituents to the generated artificial microstructure models with various statistical input parameters of grain size distribution function, the influence of the grain size distribution on the strain hardening behavior of the dual phase materials can be fully investigated.

REFERENCES

[1] Ghosh S., Micromechanical analysis and multi-scale modeling using the Voronoi cell finite element method. CRC Press, Taylor & Francis Group, 2011.
[2] Okabe A., Boots B., Sugihara K., Chiu S.N., Spatial Tessellations: Concepts and Applications of Voronoi Diagrams, Second Edition, John Wiley & Sons Inc. 1992, 2000.
[3] Franklin F.J., Gahlot A., Fletcher D.I., Garnham J.E., Davis C., Three-dimensional modelling of rail steel microstructure and crack growth, Wear 2011; 271: 357-363.
[4] Nygards M., Gudmundson P., Three-dimensional periodic Voronoi grain models and micromechanical FE-simulations of a two-phase steel, Computational Materials Science 2002; 24: 513-519.
[5] Regener B., Krempaszky C. Werner E., Stockinger M., Modelling the micromorphology of heat treated Ti6Al4V forgings by means of spatial tessellations feasible for FEM analyses of microscale residual stresses, Computational Materials Science 2012; 52: 77-81.
[6] Aurenhammer F., Edelsbrunner H., An optimal algorithm for constructing the weighted Voronoi diagram in the plane, Pattern Recognition 17 1984, No. 2: 251-257.
[7] Mukherjee K., Hazra S., Militzer M., Grain refinement in dual-phase steel. Metall. Mater. Trans. 2009; 40: 2145–2159.
[8] MATLAB R2012b documentation. Version R2012b. The MatWorks Inc.
[9] Crow E.L., Shimizu K., Lognormal distributions: theory and applications. Marcel Dekker Inc., 1988.
[10] Tarjus G., Schaaf P., Talbot J., Random sequential addition: A distribution function approach. JSP 1991; 63: 167-202.
[11] Toquato S., Random heterogeneous materials. Springer-Verlag Inc., 2002.
[12] Roters F., Overview of constitutive laws, kinematics, homogenization and multiscale methods in crystal plasticity finite-element modeling: theory, experiments, applications, Acta Mater. 2010; 58 : 1152-1211.
[13] Tikhovskiy I., Raabe D., Roters F., Simulation of Earing of a 17% Cr Stainless Steel Considering Texture Gradients, Mat. Sci. Eng. a-Struct 2008; 488: 482-490.
[14] Wang Y., Orientation dependence of nanoindentation pile-up patterns and of nanoindentation microtextures in copper single crystals, Acta Mater. 2004; 52: 2229-2238.
[15] Helm D., Microstructure-based description of the deformation of metals: theory and application, JOM 2011; 63: 26-33.

[16] Butz A., On the modeling of dual phase steels: microstructure-based simulation from the hot rolled sheet to the deep drawn component, Int. J. Mater. Form. 2010; 3: 73-76.
[17] ABAQUS/Analysis user's manual. Version 6.12. ABAQUS Inc.
[18] Lian J., Gao S., Sharaf M., Vajragupta N., Schmaling B., Ma A., Münstermann S., Hartmaier A., Bleck W., Crystal plasticity modelling on single crystal and polycrystal of a ferritic steel sheet, In: Proceeding of Materials Science and Technology 2012 Conference, Pittsburgh, USA.
[19] Pickering FB. Constitution and properties of steels, vol. 7. In: Cahn RW, Haasen P, Kramer EJ, editors. VCH Publishers Inc., New York, NY, USA; 1992.
[20] Samek L., De Cooman B.C., van Slycken J., Verleysen P., Degrieck J., Physical metalllurgy of multi-phase steel for improved passenger car crash-worthiness, Steel Res. Int. 2004; 75: 716-724.
[21] Rodriguez R.M., Gutierrez I., Unified formulation to predict the tensile curves of steels with different microstructures, Mater. Sci. Forum 2003; 426-432: 4525-4530.
[22] Rodriguez R.M., Gutierrez I., Mechanical behaviour of steels with mixed microstructures, In: Proc. of the 2nd International conference on thermomechanical processing of steels (TMP'2004), Liege; 2004.
[23] Reisner G., Werner E.A., Fischer F.D., Micromechanical modelling of martensitic transformation in random microstructures, Int. J. Solids Struct. 1998; 35: 2457-2473.